The astrochemical factory: A solid base for interstellar reactions

Ligterink, N.F.W.

V-UV

$CO{:}CH_3OH(s) \rightarrow CO(g) + CH_3OH(g)$

$CH_3CHO(s)$

$CH_3OCH_3(s)$ $CH_3CH_2OH(s)$

$CH_3(s) + NCO(s) \rightarrow CH_3NCO(g)$

10

$CH_3 + NH_2CO \rightarrow CH_3CONH_2$

$CH_3NH_2(g)$

$CH_2NH + H \rightarrow CH_3NH_2$

$NO + H \rightarrow NH_2OH$

$H + Br \rightarrow HBr$

Interstellar bromine depletion matches cometary ices from *Rosetta*

N.F.W. Ligterink & M. Kama

Ligterink & Kama 2017, *Interstellar bromine depletion matches cometary ices from* Rosetta, subm. to A&A

10.1. Introduction

Observations of halogen-bearing species in molecular gas can probe the gas-to-ice depletion of volatiles during star and planet formation and constrain the H_2 column density (Gerin et al. 2016). Previous studies have characterized the abundance of fluorine (F) and chlorine (Cℓ) in protostellar gas. We analyse archival data from the *Herschel* Space Observatory to constrain the gas-phase abundance budget of bromine (Br).

The solar abundances of F and Cℓ are $(3.63 \pm 0.11) \times 10^{-8}$ and $(3.16 \pm 0.95) \times 10^{-7}$, respectively (Asplund et al. 2009). The gas-phase HCℓ abundance in dense protostellar cores is [HCℓ/H_2]$\sim 10^{-10}$, with Cℓ depleted by a factor 100–1000 (Blake et al. 1985; Schilke et al. 1995; Zmuidzinas et al. 1995; Salez et al. 1996; Neufeld & Green 1994; Peng et al. 2010; Kama et al. 2015). Models indicate that the missing Cℓ is in HCℓ ice (Kama et al. 2015). A high Cℓ fraction in HCℓ ice was confirmed *in-situ* for comet 67P/Churyumov-Gerasimenko (hereafter 67P/C-G) with *Rosetta*, which recently measured HCℓ/$H_2O \approx 1.2 \cdot 10^{-4}$ (Dhooghe et al. 2017), close to *Herschel* upper limits at comets Hartley 2 and Garradd (Bockelée-Morvan et al. 2014).

In contrast to F and Cℓ, the solar and interstellar Br abundance is unknown, but in meteorites it is equivalent to Br/H$= (3.47 \pm 0.02) \times 10^{-10}$ (Lodders et al. 2009). The two stable isotopes of bromine are ^{79}Br and ^{81}Br, with a terrestrial abundance ratio of [^{79}Br]/[^{81}Br]=1.03 (Böhlke et al. 2005). For comet 67P/C-G, the *Rosetta* spacecraft detected HBr and measured an elemental ratio of Br/O $= (1-7) \times 10^{-6}$ in the inner coma, consistent with nearly all bromine being locked in ice, analogously to chlorine.

Accounting for the range of variation seen in 67P/C-G and the uncertainties in terrestrial data, the cometary Br/Cℓ value of ≈ 0.02 (Dhooghe et al. 2017) is consistent with the bulk Earth estimate of Br/C$\ell \approx 0.04$ (Allègre et al. 2001).

If Br has a similar depletion level as Cℓ in protostellar gas, it may be detectable as HBr at a sensitivity of $\delta T \lesssim 0.01 \times T$(HC$\ell$), where T is the intensity in kelvin. The lowest rotational transitions of HBr are at around 500, 1000, and 1500 GHz. These frequencies are not observable from the ground, but were covered by the *Herschel*/HIFI spectrometer. We also consider the potentially abundant molecular ion HBr^+. During regular science observations, HIFI serendipitously covered transitions of HBr and HBr^+ towards the bright protostellar regions Orion KL, Sagittarius B2 North – hereafter Sgr B2(N), and NGC6334I. We use these data to constrain the gas-phase abundance of Br-carriers.

In Section 10.2, we summarize the spectroscopy and the archival *Herschel* data, which are analysed and discussed in Section 10.3. In Section 10.5, we review the interstellar chemistry of Br. Our conclusions are presented in Section 10.6.

10.2. Data

10.2.1. Spectroscopy of HBr and HBr^+

Measurements on rotational lines of HBr were performed by Van Dijk & Dymanus (1969) for the hyperfine components of the first rotational transition and later extended by Di Lonardo et al. (1991) up to $J_u = 9$. The first three

Table 10.1: Source parameters in HIFI band 1a

Source	θ_S ″	RMS (mK)	$V_{\rm LSR}$ ($\rm km\,s^{-1}$)	ΔV ($\rm km\,s^{-1}$)	3σ Flux ($\rm mK\,km\,s^{-1}$)	Continuum K
Orion KL[a] Plat.	30	23.0	7 – 11	$\geq$20	364	1.6
Orion KL HC	10	23.0	4 – 6	7	216	1.6
Orion KL CR	10	23.0	7 – 9	6	200	1.6
Sgr B2(N)[b] HC	$\sim$5	29.3	50 – 100	9	311	2.5
Sgr B2(N) env.	–	29.3	50 – 100	20	464	2.5
NGC6334I[c] HC	$\sim$5	7.8	-20 – 7	4	55	1.0
NGC6334I env.	20*	7.8	-20 – 7	8	78	1.0

Notes. Plat. – Plateau, HC – Hot Core, CR – Compact Ridge, env. – envelope. [a]Crockett et al. (2014b); [b]Neill et al. (2014); [c]Zernickel et al. (2012); *based on the derived HCℓ source size.

rotational transitions of both $H^{79}Br$ and $H^{81}Br$ are found at frequencies just above 500, 1000, and 1500 GHz, respectively (Table 10.4 in the Appendix). The three lowest rotational transitions of HBr^+ are found at 1188.2, 1662.7 and 2136.8 GHz and also display hyperfine splitting (Saykally & Evenson 1979; Lubic et al. 1989). However, insufficient spectroscopic data of HBr^+ are available to determine column densities. The lowest HBr and HBr^+ transition frequencies fall in spectral regions with heavy atmospheric absorption and are best observed from space.

10.2.2. Archival *Herschel* observations and selected sources

The *Herschel* Space Observatory mission (Pilbratt et al. 2010), active from 2009 to 2013, was the most sensitive observatory to date in the terahertz frequency range. We investigate archival high spectral resolution and broad wavelength coverage data from its heterodyne instrument, HIFI (de Graauw et al. 2010).

The HEXOS guaranteed-time key program (PI E.A. Bergin, Bergin et al. 2010) obtained full spectral scans of Orion KL and Sgr B2 (Crockett et al. 2014b,a; Neill et al. 2014), covering three rotational transitions of HBr in HIFI bands 1a, 4a and 6a and HBr^+ transitions in band 5a and 6b. The CHESS key program (PI C. Ceccarelli, Ceccarelli et al. 2010) observed NGC6334I in the same HIFI bands (Zernickel et al. 2012). These three sources are bright and well-studied, and have yielded strong detections of the halogens HF and HCℓ ($\int T_{mb}dv$ = 701.9 K km s^{-1} for Orion KL, $\int T_{mb}dv$ = 40 K km s^{-1} for NGC6334I). Line intensities one to two orders of magnitude lower than the HCℓ peak brightness should be detectable. The observational details of these three sources are listed in Table 10.1.

10.2.3. Analysis method

All sources are inspected for features corresponding to transitions of $H^{79/81}Br$ and HBr^+ using the `Weeds` addition (Maret et al. 2011) of the Continuum and Line Analysis Single-dish Software (CLASS[1]). For line identification, we use the JPL[2]

[1] `http://www.iram.fr/IRAMFR/GILDAS`
[2] `http://spec.jpl.nasa.gov`

(Pickett et al. 1998) and CDMS[3] (Müller et al. 2001, 2005) spectroscopy databases. Source velocities matching previous detections of halogen bearing molecules are considered most relevant, but we explore a large $V_{\rm LSR}$ range to check for emission or absorption components matching the hyperfine pattern. For emission features, the total column density $N_{\rm T}$ of the peak can be calculated by assuming local thermodynamic equilibrium (LTE):

$$\frac{3k_{\rm B}\int T_{\rm MB}dV}{8\pi^3\nu\mu^2 S} = \frac{N_{\rm up}}{g_{\rm up}} = \frac{N_{\rm T}}{Q(T_{\rm rot})}e^{-E_{\rm up}/T_{\rm rot}}, \tag{10.1}$$

where $\int T_{\rm MB}$dV is the integrated main-beam intensity, ν the transition frequency, μ^2 the dipole moment, S the strength, $g_{\rm up}$ the upper state degeneracy, $Q(T_{\rm rot})$ the rotational partition function, $E_{\rm up}$ the upper state energy and $T_{\rm rot}$ the rotational temperature. Upper limits are given at 3σ confidence and calculated by $\sigma = 1.1\sqrt{\delta\nu\Delta V}\cdot$RMS, where $\delta\nu$ is the velocity resolution, ΔV the line width (estimated based on other transitions in the spectrum) and RMS the root mean square noise in Kelvin. A factor of 1.1 accounts for the flux calibration uncertainty of 10% (Roelfsema et al. 2012).

In the source sample, the hydrogen halides HF and HCℓ are also found in absorption. We calculate the column density corresponding to absorption features by:

$$\tau = -ln\left(\frac{T_{\rm MB}}{T_{\rm cont}}\right) \tag{10.2}$$

and

$$N_{\rm T} = \frac{8\pi^{3/2}\cdot\Delta V}{2\sqrt{ln2}\cdot\lambda^3}\frac{g_{\rm l}}{g_{\rm u}}\cdot\tau, \tag{10.3}$$

where τ is the optical depth, $T_{\rm MB}$ the brightness temperature of the feature and $T_{\rm cont}$ the continuum level. λ is the wavelength of the transitions and $g_{\rm l}$ and $g_{\rm u}$ are its lower and upper state degeneracies. For non-detections, a 3σ upper limit column density is determined by using $T_{\rm MB}$ = $T_{\rm cont}$-3·RMS and assuming ΔV equals the average line width for other species in the source.

If the source does not fill the entire HIFI beam (at 500 GHz, $\theta_{\rm B}$=44″), we correct the column densities for beam dilution by applying the factor $\eta_{\rm BF} = \theta_{\rm S}^2/(\theta_{\rm S}^2+\theta_{\rm B}^2)$, where $\theta_{\rm S}$ is the source size and $\theta_{\rm B}$ the beam size. Source sizes are taken from literature, see Table 10.1. The *source*-averaged column density is calculated from $N_{\rm S} = N_{\rm T}/\eta_{\rm BF}$.

To make use of the best noise levels, we determined the upper limit column densities for the HBr J = $1_x \rightarrow 0_2$ transitions at 500 GHz in HIFI band 1a. In HBr, we consider the sum of H^{79}Br and H^{81}Br. We assume that the cosmic and local isotope ratios are equal (in the solar system [^{79}Br]/[^{81}Br]=1.03). Aside from the molecular mass, several spectroscopic parameters for transitions of both isotopes, such as $A_{\rm ij}$ and $E_{\rm up}$, are identical. The $1_3 \rightarrow 0_2$ line constrains the column density the most and is therefore used to give the most stringent upper limits.

[3] `http://www.astro.uni-koeln.de/cdms`

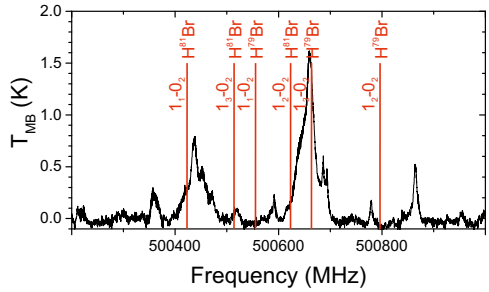

Figure 10.1: Positions of the J = $1_x \rightarrow 0_2$ transitions of $H^{79}Br$ and $H^{81}Br$ at 500 GHz towards Orion KL for V_{LSR} = 9 km s^{-1}.

10.3. Search for HBr and HBr^+ in the *Herschel* spectra

Analysis of the HIFI spectra of Orion KL, Sgr B2(N) and NGC6334I yielded no detections of HBr or HBr^+ features in emission or absorption. Figure 10.1 shows the positions of the HBr transitions at 500 GHz in the Orion KL spectrum at V_{LSR} = 9 km s^{-1}. The data were analysed over a large range of source velocities, mainly focussing on velocities of known components. For Sgr B2(N) and NGC6334I the same figures can be found in Appendix 10.7.2.

10.4. Protostellar *vs* cometary abundance

The upper limit abundance ratios of HBr toward the protostellar sources can be compared with measurements taken by the *Rosetta* mission of the coma gas of comet 67P/C-G (Dhooghe et al. 2017). We look at column density ratios of HBr (Table 10.5) with respect to that of H_2, H_2O, CH_3OH, HF, and HCℓ (Table 10.6). The $N(H^{79+81}Br)/N(X)$ column density ratios based either on emission or absorption upper limits for Orion KL, Sgr B2(N), and NGC6334I are listed in Table 10.2.

The upper limits in emission are based on an excitation temperature of 100 K, which is chosen to be within a factor of a few of all the detected molecules we compare with. For an assessment of the impact of T_{ex}, Fig. 10.6 shows the temperature dependence of the 3σ upper limit for the first three hyperfine transitions of $H^{79/81}Br$, including beam dilution correction for the Orion KL Hot Core. For Sgr B2(N) and NGC6334I a distinction is made between the hot core and envelope components. If a source contains multiple kinematic components of a species, we adopt the dominant one.

For 67P/C-G, Dhooghe et al. (2017) give the Br/O ratio and the CH_3OH abundance. The cometary halogens are equal to the halides (HX), but the O abundance is the sum of H_2O, CO, CO_2 and O_2. For the comet, we can therefore take Br≡HBr, and we further assume O≈H_2O. A ratio of CH_3OH/H_2O = 3.1–5.5×10^{-3} has been measured by Le Roy et al. (2015).

A comparison of HBr with H_2O and CH_3OH is shown in Fig. 10.2, and the full set of abundance ratios of HBr with other molecules is given in Table 10.2. The HBr/CH_3OH ratio in all our targets is constrained to be below that in comet

Table 10.2: Abundance ratios of $H^{79+81}Br$ (≡B) upper limit column density with H_2, CH_3OH, H_2O, HF, and $H^{35+37}C\ell$(≡HCℓ) for Orion KL, Sgr B2(N) and NGC6334I, compared with abundance ratios derived for 67P/C-G

Source	B/H_2	B/H_2O	B/CH_3OH	B/HF	B/HCℓ
Orion KL Plat.[a]	$\leq 8.9\times10^{-11}$	$\leq 1.9\times10^{-5}$	–	$\leq 1.2\times10^{1}$*	$\leq 1.3\times10^{-2}$
Orion KL HC[a]	$\leq 3.1\times10^{-10}$	$\leq 4.8\times10^{-7}$	$\leq 1.4\times10^{-4}$	–	–
Orion KL CR[a]	$\leq 2.3\times10^{-10}$	$\leq 4.9\times10^{-5}$	$\leq 1.9\times10^{-4}$	–	–
Sgr B2(N) HC[b]	$\leq 6.5\times10^{-11}$	$\leq 1.0\times10^{-2}$	$\leq 1.0\times10^{-4}$	–	–
Sgr B2(N) env.[b]	–	–	$\leq 1\times10^{-3}$	$\leq 1.1\times10^{-1}$*	$\leq 6.9\times10^{-2}$*
NGC6334I HC[c]	$\leq 8.4\times10^{-11}$	$\leq 4.4\times10^{-5}$	$\leq 6.6\times10^{-6}$	–	$\leq 4.8\times10^{-1}$
NGC6334I env.[c]	–	–	–	$\leq 2.0\times10^{-1}$*	$\leq 9.3\times10^{-1}$*
67P/C-G[a]	–	$4.5^{+3.5}_{-3.5}\times10^{-6}$ [b]	$1.4^{+1.2}_{-0.7}\times10^{-3}$	$1.7^{+5.1}_{-1.3}\times10^{-2}$	$4.8^{+13.8}_{-3.7}\times10^{-2}$

Notes. Plat. – Plateau, HC – Hot Core, CR – Compact Ridge, env. – envelope. [a]Dhooghe et al. (2017); [b]Br/O elemental ratio, O has contributions of water, but also CO, CO_2 and O_2; *indicates values based on an upper limit in absorption, other values are based on the emission upper limits.

67P/C-G. This is not necessarily due to a particularly high methanol abundance in our targets, but rather could signify a low fraction of Br atoms locked up in gas-phase HBr molecules. The only source where we can constrain the HBr/H_2O ratio to be below that in 67P/C-G is the Orion KL Hot Core. This may, again, be explained with a low fraction of Br atoms in gas-phase HBr. If all elemental bromine were in gaseous HBr, we would have expected to have made a detection in the Orion KL Hot Core. A comparison with the cometary measurements suggests, then, that the HBr molecules are formed in icy grain mantles, rather than in the gas phase, or sublimate from the grain surface at a temperature higher than water.

The HBr/HCℓ abundance ratio in the Orion KL Plateau is constrained to be a factor $\gtrsim 4$ below that in 67P/C-G. This further solidifies the interpretation of an ice-phase formation of HBr, rather than a high abundance of H_2O and CH_3OH, to explain the low upper limits on protostellar HBr/X ratios described above. We return to this interpretation from a chemical network perspective in the next section.

10.5. Interstellar chemistry of Br

The inter- and protostellar chemistry of bromine is poorly characterized, compared to that of fluorine and chlorine (e.g. Jura 1974; Blake et al. 1986; Schilke et al. 1995; Neufeld & Wolfire 2009). In Table 10.3, we present a network compiled from published measurements and calculations, with missing data filled in with values from the Cℓ and F networks.

The neutral-neutral chemistry, reactions (1) through (3), is relatively well studied. The Br+H_2 reaction leading to HBr+H, with an 8812 K activation energy, has been investigated by e.g. Eyring (1931); Plooster & Garvin (1956) and Fettis et al. (1960). The HBr+H abstraction and exchange reactions have been studied by Plooster & Garvin (1956), and by White & Thompson (1974)

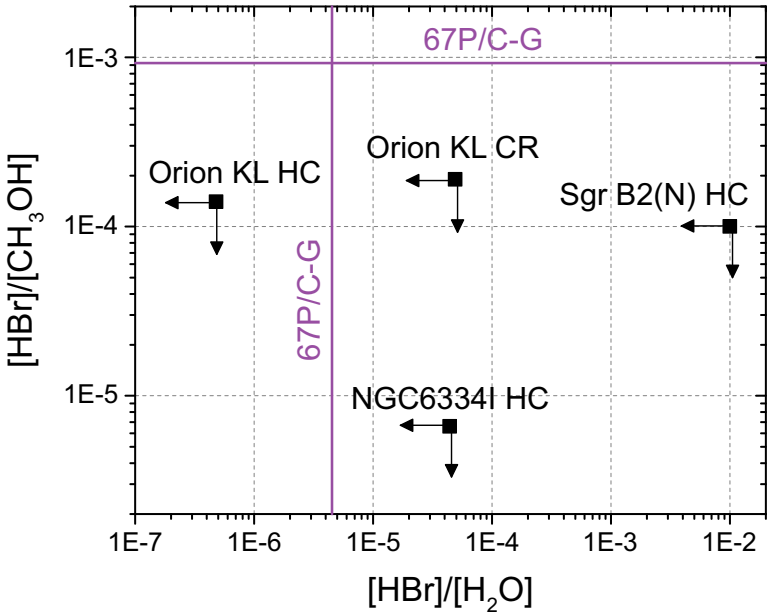

Figure 10.2: The (H)Br/CH_3OH and (H)Br/(H_2)O) ratios plotted for 67P/C-G (purple lines, Dhooghe et al. 2017) and the upper limits on these ratios for the protostar sample (this work).

whose channel-by-channel rates are consistent with the total rate from Endo & Glass (1976). Based on Table 10.3, excluding other reactions, the competition between the Br+H_2 formation route and destruction via the HBr+H abstraction reaction strongly favours atomic Br. Thus gas-phase neutral-neutral chemistry is not expected to contribute to HBr formation unless temperatures of $\sim$1000 K – possible in hot cores, outflow shocks, and inner regions of protoplanetary disks – are involved.

Due to its low first ionization potential (11.8 eV), Br is easily ionized and HBr can form in ion-neutral chemistry via the set of reactions (4)–(8) in Table 10.3. By analogy with F and Cℓ, reactions (4) through (8) should be fast, of order $10^{-10} - 10^{-7}\,cm^3s^{-1}$ (Neufeld & Wolfire 2009). However, as pointed out by Mayhew & Smith (1990), the Br^++H_2 reaction is endothermic. We adopt a H_2 and HBr^+ dissociation energy (E_D) difference of $\approx$ 6200 K, estimated from the proton affinity (PA) and ionization potential (IP) of Br via E_a=PA(Br)+IP(Br)-IP(H_2)-E_D(H_2), suggested by D. Neufeld (private communication). The branching ratio of the dissociative recombination reactions (7) and (8) is unknown, but the dissociation energy of HBr ($D_0 \approx 3.78$ eV) is lower than that of H_2 (4.48 eV), while those of HCl and HF are similar and higher (4.43 and 5.87 eV, Darwent 1970). The branching ratio into the HBr+H channel may thus be lower than the 10 % of the equivalent Cℓ reaction, which would lower the fraction of Br stored in HBr. For the photoionization and -dissociation rates, we adopt order-of-magnitude numbers from the corresponding Cℓ and F reactions in Neufeld & Wolfire (2009).

The formation of HBr via H+Br collision requires a three-body interaction and thus is most efficient on grain surfaces (e.g. Ree et al. 2004).

Table 10.3: Chemical reaction network for bromine.

#	R_1	R_2	P_1	P_2	$k(T)$ [cm^{3}s^{-1}]	Reference
(1)	Br	H_2	HBr	H	$8.3 \times 10^{-11} \times \exp(-8812\,K/T)$	Fettis et al. (1960)
(2)	HBr	H	Br	H_2	$8.9 \times 10^{-11} \times \exp(-684\,K/T)$	White & Thompson (1974)
(3)	HBr	H′	H′Br	H	$4.0 \times 10^{-10} \times \exp(-1140\,K/T)$	White & Thompson (1974)
(4)	Br^+	H_2	HBr^+	H	$10^{-9} \times \exp(-6200\,K/T)$	Mayhew & Smith (1990)[a,c] Neufeld & Wolfire (2009)[a,c]
(5)	HBr^+	e^-	Br	H	$2 \times 10^{-7} \times (T/300\,K)^{-0.5}$	Neufeld & Wolfire (2009)[a]
(6)	HBr^+	H_2	H_2Br^+	H	$(13.2 \pm 1.6) \times 10^{-10}$	Belikov & Smith (2008)
(7)	H_2Br^+	e^-	HBr	H	$\leq 10^{-8} \times (T/300\,K)^{-0.85}$	Neufeld & Wolfire (2009)[a,b]
(8)	H_2Br^+	e^-	Br	2H	$\sim 10^{-7} \times (T/300\,K)^{-0.85}$	Neufeld & Wolfire (2009)[a]
(9)	HBr	$h\nu$	Br	H	$1.7 \cdot 10^{-7} \times \chi_{UV}$	Neufeld & Wolfire (2009)[a]
(10)	HBr	$h\nu$	HBr^+	e^-	$10^{-10} \times \chi_{UV}$	Neufeld & Wolfire (2009)[a]

Notes. R_i and P_i denote the reactants and products. [a] – assumed order-of-magnitude similar to corresponding Cℓ, F reactions from Neufeld & Wolfire (2009); [b] – upper limit based on $H_2Cl^+ + e^-$ branching ratio (see text); [c] – see Section 10.5.

10.5.1. Chemical modelling results

We appended the reactions from Table 10.3 to the OSU2009 network and ran time-dependent simulations to 1.5 Myr with the `Astrochem` gas-phase chemistry code (Maret & Bergin 2015). The physical conditions were set to $A_V = 20$ mag (assuming a standard interstellar radiation field), n_{gas}=10^7 cm^{-3}, and T_{kin}=50 K. The initial halogen abundances were either entirely atomic ions (Cℓ^+ and Br^+) or entirely diatomic hydrides (HCℓ and HBr), but this had only a minor impact on the end-state abundances. We show the modelling results in Figure 10.3 for three cases: 1) all elemental Br and Cℓ in the gas-phase; 2) only Cℓ in the gas-phase and 3) both Br and Cℓ depleted from the gas by two orders of magnitude, mimicking depletion.

For the adopted physical conditions, the chemical network predictions place the gas-phase HBr abundance two orders of magnitude below the observed upper limit for the Orion KL Hot Core. All literature studies of the gas-phase Cℓ abundance in protostellar sources find gas-phase Cℓ depletions of at least a factor 100 to 1000 (Dalgarno et al. 1974; Blake et al. 1986; Schilke et al. 1995; Peng et al. 2010; Kama et al. 2015). However, the ice fraction in the Orion KL Hot Core is likely very small, so we expect model 1 to provide a reasonable prediction of the gas-phase (H)Cℓ and (H)Br abundance in this source.

In the NGC 6334I Hot Core, HBr may be just below the upper limit from *Herschel* if elemental Br is not depleted from the gas, while Cℓ is known to be depleted by a factor 1000. This seems unlikely.

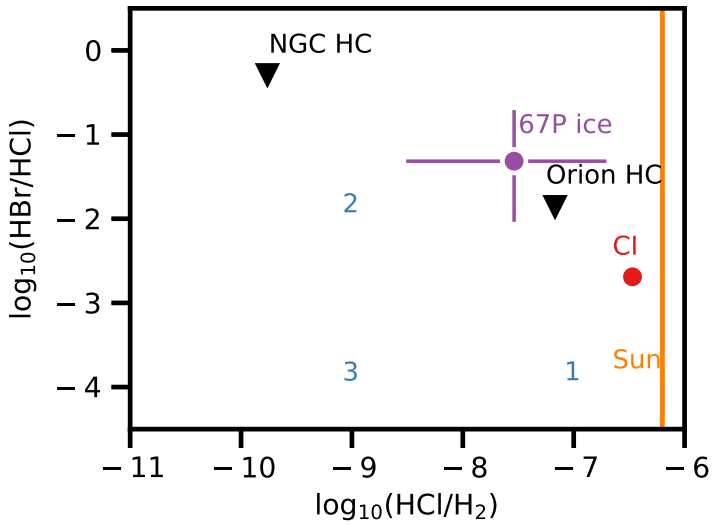

Figure 10.3: The ratio of HBr to HCℓ abundance in our protostellar sample and chemical models, and in comet 67P/C-G (Dhooghe et al. 2017). The elemental Cℓ/H_2 and Br/Cℓ ratios for meteorites and the sun are marked with $\star$. Model 1 has all elemental Cℓ and Br in the gas; in 2 only Cℓ and in 3 both Cℓ and Br are depleted from the gas by a factor of 100. See Table 10.3 for the chemical network used in the models.

10.6. Conclusions

We present the first search for bromine-bearing molecules in the interstellar medium, employing archival *Herschel*/HIFI data. No detections of HBr or HBr^+ are made, and we report upper limits of HBr for Orion KL, Sgr B2 (N) and NGC 6334I. Most of these upper limits lie above the values expected from a simple scaling down of HCℓ emission using the Cℓ/Br elemental ratio and are thus not very strong.

In the Orion KL Hot Core, the HBr/H_2O gas-phase abundance ratio is constrained to be an order of magnitude lower than the measured ratio in comet 67P/C-G. This result, along with the low HBr/CH_3OH ratio in all our sources and the low HBr/HCℓ in the Orion KL Plateau, is consistent with our chemical network modelling for Br, which suggests a high atomic fraction in the gas, and HBr formation in icy grain mantles or sublimation from the grain surface at a temperature higher than that of water.

Acknowledgement

Thanks go out to Nathan Crockett for providing the data on Orion KL and Sgr B2, and Peter Schilke for the data on NGC6334I. We also thank Frederik Dhooghe for discussing his results in before publication, David Neufeld for assistance with the chemical network, and Magnus Persson for computational

help.
MK is supported by an Intra-European Marie Sklodowska-Curie Fellowship. Astrochemistry in Leiden is supported by the Netherlands Research School for Astronomy (NOVA), by a Royal Netherlands Academy of Arts and Sciences (KNAW) professor prize, and by the European Union A-ERC grant 291141 CHEMPLAN.

10.7. Appendix

10.7.1. Linelist of HBr transitions in range of HIFI

The HIFI instrument on the *Herschel* Space Observatory covered the three lowest rotational transition groups of HBr, which are summarised in Table 10.4. J = $1_x \rightarrow 0_2$ fell in band 1a, J = $2_x \rightarrow 1_y$ in band 4a and J = $3_x \rightarrow 2_y$ in band 6a.

Table 10.4: $H^{79/81}Br$ transitions between 500 and 1501 GHz

ν $H^{79}Br$ MHz	ν $H^{81}Br$ MHz	A s^{-1}	E_{upper} K	J′,F′	J″,F″
500540.1280	500407.2010	3.34E-4	24.0	1_1	0_2
500647.7450	500497.3850	3.34E-4	24.0	1_3	0_2
500780.0980	500607.7750	3.34E-4	24.0	1_2	0_2
1000859.5610	1000589.5640	5.33E-4	72.1	2_1	1_2
1000993.2470	1000701.3110	1.71E-3	72.1	2_2	1_2
1001089.1700	1000781.6850	2.24E-3	72.1	2_3	1_2
1001089.1700	1000781.6850	3.20E-3	72.1	2_4	1_3
1001099.6240	1000790.3740	2.67E-3	72.1	2_1	1_1
1001125.5610	1000811.7800	1.60E-4	72.1	2_2	1_3
1001221.3420	1000891.7620	9.61E-4	72.1	2_3	1_3
1001233.1690	1000901.9040	1.33E-3	72.1	2_2	1_1
1500828.0700	1500397.4070	2.31E-4	144.1	3_2	2_3
1500923.7510	1500477.5790	3.24E-3	144.1	3_2	2_2
1500961.8100	1500509.4550	2.82E-3	144.1	3_3	2_3
1501025.2220	1500562.4860	9.91E-3	144.1	3_4	2_3
1501025.2220	1500562.4860	1.16E-2	144.1	3_5	2_4
1501057.6120	1500589.4380	8.10E-3	144.1	3_2	2_1
1501057.6120	1500589.4380	8.64E-3	144.1	3_3	2_2
1501094.0810	1500619.5480	1.10E-4	144.1	3_3	2_4
1501157.1420	1500672.5180	1.65E-3	144.1	3_4	2_4

10.7.2. Sgr B2(N) and NGC6334I at 500 GHz

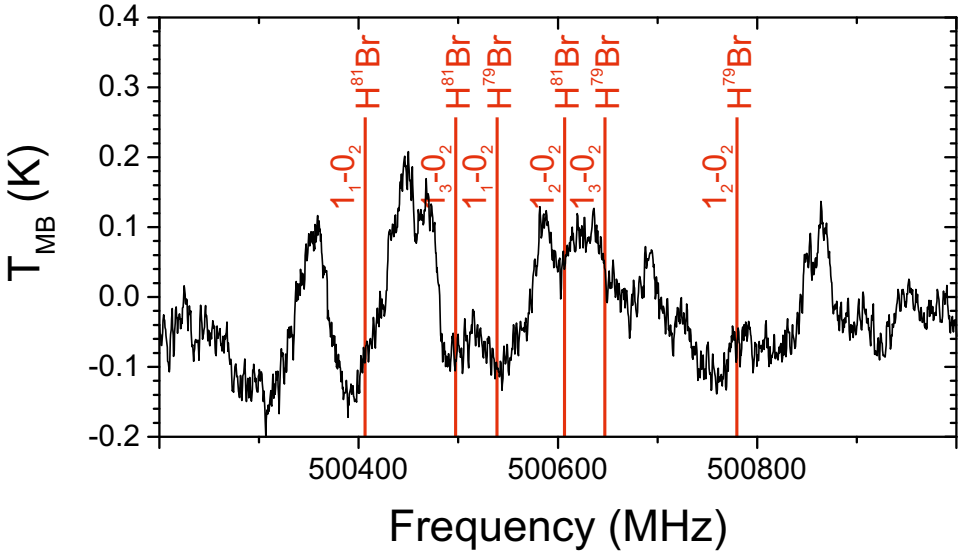

Figure 10.4: Positions of $H^{79/81}Br$ transitions for J = $1_x \rightarrow 0_2$ around 500 GHz in HIFI band 1a towards Sgr B2(N) for V_{LSR} = 64 km s^{-1}.

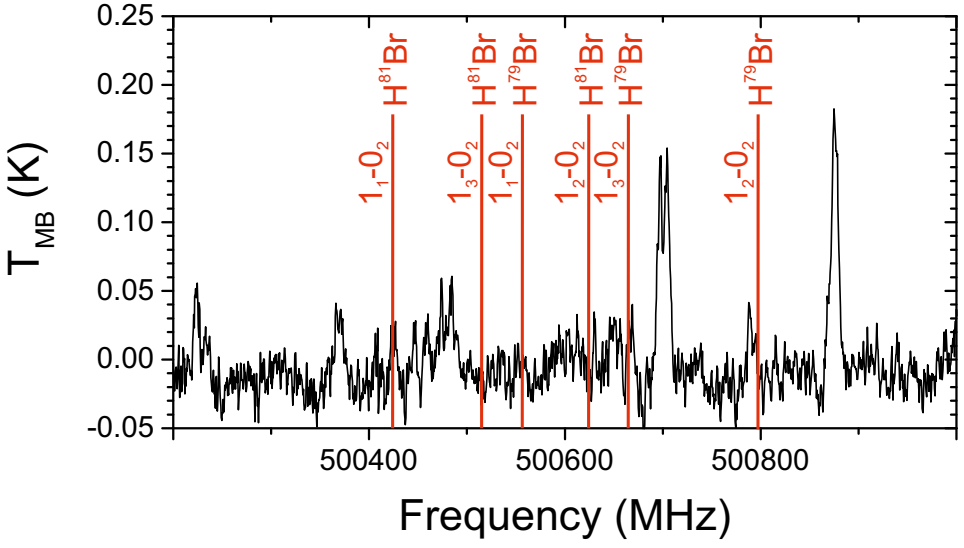

Figure 10.5: Positions of $H^{79/81}Br$ transitions for J = $1_x \rightarrow 0_2$ around 500 GHz in HIFI band 1a towards NGC6334I for V_{LSR} = -10 km s^{-1}.

10.7.3. Upper limit column densities of $H^{79+81}Br$ and column densities of reference molecules

Table 10.5 lists the upper limit column densities of $H^{79+81}Br$ for the full HIFI band 1a beam (= 44″) in emission and absorption, calculated according to Equations 10.1 and 10.3. Upper limits have been derived for an excitation temperature of 100 K. The following columns in this table list the beam dilution correction factor and subsequently the beam dilution corrected upper limit column densities.

Table 10.6 lists the column densities of the reference molecules H_2, H_2O, CH_3OH, HF, $H^{35+37}C\ell$ taken from Crockett et al. (2014b), Neill et al. (2014) and Zernickel et al. (2012).

Table 10.5: $H^{79+81}Br$ column densities and beam dilution correction

Source	$N_T(H^{79+81}Br)$ (cm^{-2})		η_{BF}	N_S	
	Emission*	Absorption		Emission*	Absorption
Orion KL Plat.	$\leq 7.9\times10^{12}$	$\leq 1.1\times10^{14}$	3.2×10^{-1}	$\leq 2.5\times10^{13}$	$\leq 3.4\times10^{14}$
Orion KL HC	$\leq 4.7\times10^{12}$	$\leq 3.8\times10^{13}$	4.9×10^{-2}	$\leq 9.6\times10^{13}$	$\leq 7.8\times10^{14}$
Orion KL CR	$\leq 4.3\times10^{12}$	$\leq 3.3\times10^{13}$	4.9×10^{-2}	$\leq 8.8\times10^{13}$	$\leq 6.7\times10^{14}$
Sgr B2(N) HC	$\leq 6.7\times10^{12}$	$\leq 4.0\times10^{13}$	1.3×10^{-2}	$\leq 5.2\times10^{14}$	$\leq 3.1\times10^{15}$
Sgr B2(N) env.	$\leq 1.0\times10^{13}$	$\leq 8.9\times10^{13}$	–	–	–
NGC6334I HC	$\leq 1.2\times10^{12}$	$\leq 1.2\times10^{13}$	1.3×10^{-2}	$\leq 9.2\times10^{13}$	$\leq 9.2\times10^{14}$
NGC6334I env.	$\leq 1.7\times10^{12}$	$\leq 2.4\times10^{13}$	1.7×10^{-1}**	$\leq 1.0\times10^{13}$	$\leq 1.4\times10^{14}$

Notes. *Emission at T_{ex} = 100 K; **Beam dilution factor based on HCℓ source size.

Table 10.6: Column densities of the reference molecules H_2, H_2O, CH_3OH, HF, $H^{35+37}C\ell$

Source	H_2	H_2O	CH_3OH (cm^{-2})	HF	$H^{35+37}C\ell$
Orion KL Plat.[a]	2.8×10^{23}	1.3×10^{18}	-	2.9×10^{13}*	1.9×10^{15}
Orion KL HC[a]	3.1×10^{23}	2×10^{20}	6.8×10^{17}		
Orion KL CR[a]	3.9×10^{23}	1.8×10^{18}	4.7×10^{17}		
Sgr B2(N) HC[b]	8×10^{24}	5-10$\times10^{16}$	5×10^{18}		
Sgr B2(N) env.[b]	-	-	1×10^{16}	8.2×10^{14}*	1.3×10^{15}*
NGC6334I HC[c]	1.1×10^{24}	2.1×10^{18}	1.4×10^{19}	-	1.9×10^{14}
NGC6334I env.[c]				1.2×10^{14}*	1.5×10^{14}*

Notes. [a]Crockett et al. (2014b), [b]Neill et al. (2014) [c]Zernickel et al. (2012) and references therein; *absorption component

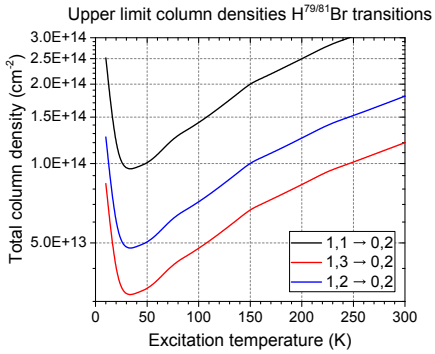

Figure 10.6: Upper limit column densities for the $H^{79/81}Br$ (e.g. ^{79}Br and ^{81}Br are used interchangeably here) J = $1_x \rightarrow 0_2$ transitions plotted versus rotational temperature based on the 3σ values (216 mK km s^{-1}) found for the Orion KL Hot Core and beam-dilution corrected (η = 0.049)